ISSN 0915-633X

NATIONAL INSTITUTE FOR FUSION SCIENCE

Simulation Study of Scalings in Scrape-Off Layer Plasma by Two Dimensional Transport Code

S.-I. Itoh, N. Ueda and K. Itoh

(Received – Feb. 26, 1990)

NIFS-24 Mar. 1990

RESEARCH REPORT
NIFS Series

NAGOYA, JAPAN

Simulation Study of Scalings in Scrape-Off Layer Plasma by Two Dimensional Transport Code

Sanae-I. Itoh, Noriaki Ueda* and Kimitaka Itoh

National Institute for Fusion Science, Chikusaku, Nagoya 464-01

*Mitsubishi Atomic Power Industries, Inc., Shibakoen, Minatoku, Tokyo 105

Japan

Abstract

Numerical analysis on Scrape-Off Layer (SOL) plasma and divertor plasma in tokamaks is made by using two-dimensional time-dependent transport code (UEDA code). Plasma transport in SOL and the divertor region is calculated for given particle and heat sources from the main plasma. Scaling study of the density, the temperature and their fall-off lengths is done for JFT-2M tokamak. The results show us inter-relations between the divertor plasma parameters and the core plasma confinement. The operational conditions of the core to guarantee the divertor performance are discussed.

key words: tokamak, 2D-transport, scaling, SoL, divertor

1. Introduction

Recently, important roles of Scrape-off Layer (SOL) and divertor plasmas for a core plasma confinement have been recogi-nized. The basic process in SOL and divertor region has been widely studied (Yoshikawa et al., 1963; Uehara et al., 1979; Post and Behrisch, 1984; Nuehauser et al., 1989). The study on the one-dimensional (1-D) structure along the field line has enabled us to do the quantitative comparison with experimental observations (Harbour and Morgan, 1983; Neuhauser, et al., 1984). In these studies, multi-ion fluid plasma has been examined and the importance of the parallel electric field and of thermal forces has been shown. However the width of the SOL plasma should be given as a parameter. The 2-D structures with respect to the poloidal asymmetry have been also attracted attentions in studying phenomena of SOL and divertor plasmas.

The 2-D SOL transport model and codes for single ion plasma have been extensively developed (Petravic, et al., 1982; Braams, 1983; Petravic, et al., 1984(a); Petravic ,et al., 1984(a); Igitkhanov, et al., 1985; Braams et al.,1986). Multi-fluid 2-D modelling has recently been developed (Braams, 1987) to study the transport of helium ash and impurities through the edge plasma. There, fluids equations are used with different ion and electron temperatures. The currentless flow is assumed with the charge neutrality condition. Plasma interactions are included in terms of ionization and recombination processes, interspecies friction, electric and thermal force and temperature equilibra-tion. The neutral particles are treated by an analytical model.

In order to follow a particle behavior, a Monte Carlo model has successfully been applied to the 2-D impurity transport analysis. A particle model has been shown to be a useful tool to examine the ash and impurity transport (Brooks, 1987). Combining the 2-D transport code with a Monte Carlo method for neutrals, the time independent PLANET code (Petravic. et al., 1982; 1984(a); 1984(b); 1985) and time dependent Unified Edge Divertor Analysis code has been developed (Ueda, et al., 1988).

On the other hand, in the study of H-mode (Wagner et al., 1982), it has been found that the relative direction of the null point to the ion ∇B-drift velocity affects the plasma confinement (Hinton, 1985; Wagner et al., 1985; Stott,et al., 1988). Theories have been developed to show that the direction of magnetic field line influences the heat flux (Hinton, 1985; Hinton, 1988). This is also the 2-D problem of SOL plasma.

Transport of the SOL plasma correlates with both the core and divertor plasmas; the power and particle scaling-study is necessary to have an unified picture of plasma confinement and of divertor plasma. Namely, the plasma density and temperature in divertor region are sustained by the heat and particle fluxes from the core, and they affect the multiplication of the neutral particles, the pumping rate, the erosion rates, the back-flow rates of impurities, the radiative cooling rate and so on. In turn, in a stationary state, the edge temperature and density in SOL plasma dictate the boundary conditions for the core plasma profiles.

The UEDA code has been applied to obtain the minimum dis-

tance between the limiter head and plasma surface to prevent SOL plasma - wall interaction (Ueda, et al., 1989(a)). Concerning a diamagnetic effect due to the toroidal magnetic field direction, drift heat flux which is proportional to $B \times \nabla T_i$ (Leduc - Righi effect in thermoelctronics) has been incorporated. This effect has been found to change the heat channel width near the null-point and divertor region (Ueda, et al., 1989(b)).

In this paper we consider the single-null divertor plasma in JFT-2M tokamak. Using the model transport coefficients of SOL plasma, the scaling relation of the boundary to the divertor plasma is studied. We solve the 2-D structure, where the width of heat flux channel, motions of neutral particles in a realistic geometory of the chamber and changes of plasma parameters in SOL are calculated in a consistent manner. The 2-D effect is analyzed and the results are compared with the theoretical estimate. Based on the obtained scalings, we consider the mutual constraints between the core plasma and the divertor plasma.

The outline of this paper is as follows. In Sec.2, we briefly describe our simulation model. The description of physical and numerical content of UEDA code is shown together with boundary conditions. In Sec.3, simulational results on the scaling study of transport in SOL are shown. Analysis on the constraint for establishing "dense and cold" divertor condition is done. Summary and discussions are given in Sec.4.

2. Simulation Model

A model geometry of SOL and divertor region simulates JFT-2M tokmak configuration. The poloidal crosssection with a domain of the calculation is shown in Fig.1. Machine parameters are; major radius R = 1.31 m, minor radius a = 0.35 m, b = 0.53 m and B_T = 1.4 T. The toroidal symmetry is assumed. The orthogonal coordinates ψ and z, which correspond to the poloidal flux and length of magnetic field line projected on the poloidal crosssection, are employed. The region of calculation is divided into cells (i,j), where i and j denote the cell number in the z and ψ directions. The poloidal arc length of the divertor ℓ is measured along the plate on the crosssection. The ratio of B_p to B_t is also shown as a function of the poloidal angle. The direction of the toroidal magnetic field is defined as clock-wise (CW) and counter-clock-wise (CCW) as shown in Fig.1. The case CCW corresponds to that where the ion ∇B-drift is toward the x-point. In this paper, we analyse CCW case unless specified.

In the domain, the multi-fluid equations and neutral gas motion are solved. The motion of the neutral particle is calculated by the Monte-Carlo code, DEGAS(Heifets, 1982). A set of multi-fluid equations consists of the continuity equation for the density, the momentum conservation equation governing parallel velocity $v_{\parallel}$, and the energy equations for electrons and ions. The cross field particle flux is due to the anomalous diffusion in the presence of the density gradient. The charge neutrality is assumed and the flow is currentless. The electron inertia terms are neglected. The present analysis consider a single

average ion fluid. The kinetic energy consists of that from parallel flow, that from perpendicular diffusion and iostropic temperatures. Each temperature is denoted by T_e or T_i, for electrons or ions, respectively.

The transport coefficients we use are the classical conductivities for the parallel direction, $\kappa_\parallel$ (Braginskii,1965), and the Bohm-type anomalous diffusion ($D_\perp$) and conduction ($\kappa_\perp$) coefficients for the perpendicular direction. The observation of Bohm-like dependence of $D_\perp$ has been reported in JET experiments. (Tagle et al., 1987; Erents et al., 1988) We adopt the numerical coefficients of $D_\perp$ and $\kappa_\perp$ after the comparison study with D-III experiments (Ueda et al.,1988) as $D_\perp = D_B/2$ and $\kappa_\perp = 2nD_B$. The viscosity is neglected, therefore only diagonal elements of stress tensor are retained. At present, electric field force is only due to the thermoelectric field. The diamagnetic effect is included in the heat fluxes of electrons and ions as,

$$q = -\kappa_\perp \nabla_\perp T - \kappa_\parallel \nabla_\parallel T + \kappa_\Lambda \vec{b}\times\nabla T, \qquad (1)$$

$$\kappa_\Lambda = \sigma 5nT/2eB_T$$

where $\vec{b} \equiv \vec{B}/B$. We take $\sigma = -1$ for electrons. The conductivity coefficients, $\kappa_\parallel$ and κ_Λ, are taken from Braginskii(Braginskii, 1965). Coupling between species takes place via ionization and recombination processes, temperature equilibration and thermal forces. Frictional force is neglected. Detail of fluid equation in UEDA code other than the heat flux terms has been reported (

Ueda, et al., 1988), and we do not repeat here.

At the plasma edge, the particle (mass) and the energy input to the SOL, i.e., the output from the core, are given. In UEDA code, the total particle flux, Γ_{out}, and the total energy fluxes of electrons and ions , Q_e and Q_i, are parameters. (Γ_{out} and $Q_{e,i}$ are the values integrated on the plasma surface, and $P_{out} = Q_i + Q_e$) We assign the mass and the energy to the boundary cells in SOL. The method for the poloidal distribution is given in previous report(Ueda et al., 1989(b)). In the following we assume $Q_e = Q_i$. These values reflect the confinement times of partilce (τ_p) and energy (τ_E) in the core plasma.

As the boundary conditions close to the divertor plate, we impose the following conditions at the magnetic sheath. Because the magnetic field lines are oblique to the divertor plate (the angle, ϕ, is 5° to 10° from the plate), we consider the magnetic sheath region in addition to the electric sheath. (Chodura, 1982; Chodura, 1984). The sum of the thickness of the sheaths amounts to 4 ~ 5 times ion gyroradius, being very thin in comparison with the mesh of our fluid calculation. Therefore we consider that the surface of the magnetic sheath is our calculating boundary. At the magnetic sheath, we use Chodura's sheath condition on the momentum,

$$v_{\parallel} = \sqrt{(T_e + T_i)/m_i}, \qquad (2\text{-}1)$$

and conditions,

$$\nabla_{\parallel} T_e = -C_e n_e v_{\parallel} T_e / \kappa_{\parallel e}, \quad (C_e = 1.8) \qquad (2\text{-}2)$$

$$\nabla_{\parallel} T_i = 0. \qquad (2\text{-}3)$$

for electron and ion energy fluxes. Taking the value of C_e=1.8 in (2-2) corresponds to the case where we neglect the secondary electron emission. The condition (2-3) corresponds to an assumption that the ion conduction part is set to be zero at the interface between presheath and the sheath. The neglection of conductive part gives an independent constraint to the effect of the inclination of the magnetic field line. This assumption by no means is general, but is at least consistent to our numerical results. The transmission coefficient, γ, has the angle, ϕ, dependence of the inclined magnetic field. The neglection of the secondary emission of electrons affects the coefficient, γ, as well as the value of sheath potential.

In our case where the inclination of magnetic field line to the divertor plate is very small (5 to 10 degrees), the effect on the heat transmission coefficient and on the magnitude of the sheath potential, owing to the neglect of secondary emission, is small (Chodura 1984). We adopt the constant heat transmission coefficient γ to be 4.8. The value corresponds to the case of $\phi=10^{\circ}$. For the same fluxes, Q and Γ, at the divertor, the case of $\phi=5^{\circ}$ ($\gamma\simeq4.2$ and C_e=1.8) will show a little higher electron temperature. The deviation is at most 10%.

The particle flux at the sheath is also affected by the secondary emission of electrons. The neglection causes the underestimate of the electron density. In the present case ($5^{\circ}<\phi<10^{\circ}$) with the same fluxes at the sheath, electron density will

increase by 50% (or factor 3) and the electron temperature will decreases by 10% (or ∿25%), when the coefficient of the secondary emission is increased to be 0.5 (or 0.8). The neglection of secondary emission comprises the extra loss of electrons transferred to ions in the succeeding Debye region, this, in turn, causes an extra momentum input for ions, which causes a bulk flow. The effect in the presence of the arbitrary inclination of magnetic field line and the choice of the boundary conditions (2-2) and (2-3) are discussed in the final section.

Numerical method for the dynamic fluid equations is the particle-in-cell (PIC) method (Harlow et al., 1965). Details of the method are reported elsewhere (Ueda, et al., 1988 ; Ueda and Tanaka, 1989(c)), and are not repeated here. The behavior of the neutral gas is calculated with a Monte Carlo method (DEGAS code), using the same mesh in the fluid calculation but in real space. In order to save the computation time, the neutral gas calculation is performed once every few tenths of the time for fluid calculation cycle. As for the coupling procedure and smoothing techniques are also reported. (Ueda, et al., 1988)

The material of the first wall and the divertor plate is considered to be iron (SUS). Therefore, Marlow model included in the DEGAS (version 45) is employed for the reflection model. Furthermore, no particle pumping is assumed in the actual calculations.

3. Results and Applications

-- Scaling Study of Transport in SOL --

The simulation is performed to obtain inter-relation of the edge plasma and the divertor plasma. Using the total particle flux, Γ_{out}, and the heat flux, P_{out}, from the core as parameters, we study the dependences of the edge density (n_b), the density fall-off length (λ_n), the electron temperature ($T_{b,e}$) and its fall-off length (λ_T) (measured at the mid-plane), as well as the density and the electron temperature at the divertor plate, n_d and $T_{d,e}$. The electron temperature is depicted, since T_b and T_d of electrons are important parameters which dictate the core transport and the sheath condition near the divertor, respectively. The temperature has a profile along the divertor plate, and T_d represents the peak value on the plate. The localtions of measured points are shown in Fig.2(a). The measurements are done in a state, where the multiplication of the neutrals becomes saturated in time in the absence of active pumping. Independent of divertor plasma temperature, the dense divertor plasma can be established when the high recycling condition, i.e., the multiplication of the neutrals is sufficient. We do the simulation in parameter ranges where the dense divertor plasma condition holds.

The parameter range of Γ_{out} is from 2×10^{21}/sec to 9×10^{22} and that of P_{out} is from 0.2 MW to 0.9 MW as is shown in Fig.2(b). We have obtained the result from our calculations that the absolute value of electron temperature at the divertor scales as $T_{d,e} = 30P_{out}(MW)\Gamma_{out}(10^{22}/sec)$ eV in this configuration. There-

fore, the choice of parameters is done such that the expected $T_{d,e}$ is roughly from 15 eV to 75 eV. In this range of parameter, we can examine whether the cold divertor condition is satisfied or not in the presence of dense plasma. In the following, we may define the "cold divetor plasma" as $T_{d,e} < 10 \sim 20$eV. Importance of the cold divertor temperature is well known, since above such temperature, the erosion rates can strongly increase. For the divertor design of next generation tokamaks like a ITER, for example, this condition is serious and important(ITER Team, 1989; Itoh, et al., 1989). Furthermore, if the divertor temperature is high, it is difficult to sustain the temperature difference between $T_{b,e}$ and $T_{d,e}$. Then the shielding effect on sputterd impurities due to the temperature gradient along the field line decreases (Igitkhanov, et al., 1985), which may cause the back flow of impurities into the core plsma region.

The results on n_b, $T_{b,e}$, n_d and $T_{d,e}$ are shown in Figs. 2(c), 2(d), 2(e) and 2(f), respectively. Namely, we find near the plasma boundary,

$$n_b \propto \Gamma_{out}{}^{1} P_{out}{}^{-0.3}, \qquad (3\text{-}1a)$$

$$T_{b,e} \propto \Gamma_{out}{}^{-0.25} P_{out}{}^{0.5}. \qquad (3\text{-}1b)$$

We see that the reduction of particle flux yields the decrease of the edge density and the moderate increase of the temperature for the fixed output power. We also obtain the dependences of λ_n and λ_T as

$$\lambda_n = d\,\Gamma_{out}^{-0.24} P_{out}^{0.15}, \qquad (3\text{-}1c)$$

$$\lambda_T = d\,\Gamma_{out}^{0.4} P_{out}^{-0.23} \qquad (3\text{-}1d)$$

where the value of d is 1.8 cm in JFT-2M for $\Gamma_{out} = 10^{21}$/sec and P_{out} = 100kW. Note that the power and the particle dependences of λ_n and λ_T are different from each other. The density fall-off length expands while the heat channel contracts with the higher power flux for given Γ_{out}. Eliminating the power dependences between (3-1a) and (3-1c) and between (3-1b) and (3-1d) we obtain $n_b \lambda_n^2 \propto \Gamma_{out}^{0.5}$ and $T_{b,e} \lambda_T^{2.2} \propto \Gamma_{out}^{0.63}$. These relations imply that the strong change in particle outflux causes the moderate changes in the fall-off lengths even for the fixed edge density and temperature. This should be compared with the recent experiment in ASDEX, where the scrape-off length is not so sensitive to the change of the confinements from saturated ohmic (SOC) to improved ohmic (IOC)(McCormick et al., 1989).

Our results are compared with the Lackner-Wagner (L-W) scaling(Wagner and Lackner, 1984). The L-W scaling is obtained by using Bohm-like κ and the classical parallel transport coefficients, and by assuming the time scale separation between the parallel and the perpendicular diffusions. The viscous effect is neglected. The coefficients we use here are similar to theirs, and we include the 2-D effect and neutral behavior in our simulation. The L-W scaling shows that edge temperature, T_b, scales as

$$T_b^{LW} \propto P^{4/11} n_b^{-2/11} \qquad (3\text{-}2)$$

and the width of the heat channel , λ_T, is

$$\lambda_T^{LW} \propto P^{-3/11} n_b^{7/11} \text{ or } \propto n_b T_b^{\,2} P^{-1}. \qquad (3\text{-}3)$$

From our simulation, we obtain T_b and λ_T at the midplane, eliminating Γ in Eq.(3-1),

$$T_{b,e} \propto P^{0.4} n_b^{-0.25} \qquad (3\text{-}4)$$

$$\lambda_T \propto P^{-0.11} n_b^{0.39} \qquad (3\text{-}5)$$

We find a fairly good agreement in T_b, Eq.(3-2) and Eq.(3-4), even though we consider the effect of neutrals and the 2-D structure in our numerical simulation. With respect to the heat channel width, the simulation result(Eq.(3-5)) has the weaker dependence on n_b than that in Eq.(3-3). The contraction of the width at high heat flux is weaker in our simulation. This may be caused by the 2-D effect. The product $n_b T_{b,e}^{\,2.2} P^{-0.9} \lambda_T^{-1.4}$ = const. is obtained in our simulation. The L-W sacling gives $n_b T_b^{\,2} P^{-1} (\lambda_T^{LW})^{-1}$ = const.

On the divertor plate we find

$$n_d \propto \Gamma_{out}^{1.1} P_{out}^{-0.35} \qquad (3\text{-}6a)$$

$$T_{d,e} \propto \Gamma_{out}^{-1} P_{out}^{1} \qquad (3\text{-}6b)$$

It is noted that the density near the divertor plate has the close relation with the edge density. The divertor density is roughly proportional to the edge density, i.e.,

$$n_d \propto \Gamma_{out}^{1.1}/P_{out}^{0.35} \simeq (\Gamma_{out}/P_{out}^{0.3})^{1.1} \propto (n_b)^{1.1} \qquad (3\text{-}7)$$

The absolute value of the density at divertor is about twice larger than that at the midplane. The dense plasma condition in the divertor region is correlated to the edge density, i.e., the particle confinement. The cold divertor condition is also strongly affected by the outflux from the core plasma as seen in (3-6). The absolute value of the $T_{d,e}$ is $30P_{out}(MW)/\Gamma_{out}(10^{22}/sec)$ eV, having stronger dependences on Γ_{out} and P_{out} than the edge temperature has. The electron pressure $p_e = nT$ at the divertor is nearly independent of Γ_{out} and scales as $P_{out}^{0.65}$. The dependences of $p_{b,e}$ and $p_{d,e}$ differ to each other; $p_{b,e} \propto \Gamma_{out}^{0.75} P_{out}^{0.2}$ and $p_{d,e} \propto \Gamma_{out}^{0.1} P_{out}^{0.65}$. Even if the electron pressures at the edge and at the divertor have different scalings, the total pressure, $p = p_e + p_i$, is found to satisfy the relation, $p_b = 2p_d$ (Takizuka, 1989), which is usually employed in 1-D analysis.

Let us compare our results with theoretical estimate. The boundary condition on particle and heat fluxes on the divertor plate (at the magnetic sheath), which are listed in section 2 can be rewritten in a simple manner as $\overline{n}_d \overline{C}_s = \overline{\Gamma}_d/\Delta_d$, $r\overline{T}_d \overline{n}_d \overline{C}_s \propto$

$\overline{P}_d/\Delta_d$, $\overline{\Gamma}_d = \Gamma_{out}/(1-g)$ where Δ_d is the typical width of the particle and the heat fluxes at divertor, quantities with $\overline{\ }$ denote the averaged value over the plate, γ is the heat transmission coefficient and g denotes the probability of the reionization and of neutrals in the domain of calculation. Using these relations, the temperature at the divertor plate is written as,

$$\overline{T}_d = (P_{out} - P_{rad})/\gamma G\Gamma_{out} \qquad (3\text{-}8)$$

where G ($=1/(1-g)$) is the multiplication factor of the particle flux and P_{rad} is the remote radiative cooling contribution at the divertor region. In our simulation, the condition $P_{rad} << P_{out}$ is realized. When output particle, Γ_{out}, is small, i.e., the plasma density is low, the value of G is found to be an increasing function of Γ_{out}. These cases are not realized in the present analyses. As Γ_{out} becomes large in the absence of pumping, the recycling of neutrals at the divertor becomes large so as to establish the dense plasma. In these cases the value of G saturates and $G \simeq$ const. is realized in a stationary state. Measurements are done in this stage. We neglect the secondary electron emission and the value of γ is fixed to be 4.8. The temperature has the profile along the divertor plate and the profile factor, $\eta \equiv \overline{T}_d/T_{d,e}$, is around 0.5. Comparing the result of $T_{d,e}$, we have the value of G ($=2/\eta$) is around 4 and $g \simeq 0.75$. Impinging neutrals into the main plasma is simultaneously measured and the ratio to the recycled neutrals is estimated to be roughly 1-g.

We say that the particle balance is guaranteed in our simulation. There is little statistical error in DEGAS Monte Carlo calculation. From these considerations, the results of $T_{d,e}$ may be understood.

The 2-D contour plots of electron temperature and the ion density in SOL are shown in Fig.3 (a) and (b) for the case of $\Gamma_{out} = 5\times10^{21}$/sec and $P_{out} = 0.8$ MW. The maximum values of T_e and n_i are 70 eV and $5\times10^{18}/m^3$ near the mid-plane and decreases to the directions of wall and divertor. The intervals of each contour are 5 eV and $1\times10^{18}/m^3$, respectively. The current-less flow pattern is illustrated in 3(c), in which the length of the arrow shows the absolute velocity. Its scale is also shown in the figure. The neutral density profile is shown in 3(d). Two peaks of the density profile are found on the plate. The peak on the outer-side of the torus is higher. The maximum value of the contour is $8\times10^{11}/cm^3$ and is found on the divertor plate. The interval of the contour is $5\times10^{10}/cm^3$. Neutral density decreases towards the core plasma and some are impinging into the core near the separatrix. The expected D_α emmissivity is estimated by a simple formula as $D_\alpha \propto n_e n_0 T_e$ for $T_e > 5$eV after the analysis by Dylla (Dylla, 1982). This quantity is calculated by using the obtained n_0, T_e and n_e, and the relative value is shown in Fig.3(e). The 2-D profile of emmissivity is similar to that of n_0. The result of Fig.3(d) shows that the particle recycling takes place near the null-point and that the neutral particles are localized in divertor region. We find little recycling on the first wall. In this case. the cold divertor

condition, i.e., $T_d < 10 \sim 20$eV, is not satisfied. The temperature at the divertor reaches $45 \sim 50$ eV due to the large power flux in comparison with the particle flux as is expected from the scaling relation.

We prevoiously obtained the result (Ueda et al., 1989(b)) that $B \times \nabla T$ heat flux affects the width of heat channel near the divertor plate, and that the in-and-out asymmetry of divertor structure is enhanced (or reduced). However, the value of density and the temperature at the mid-plane do not show appreciable changes even we compare the CW and CCW cases. The total radiation loss and the charge exchange loss also change little. The effect of the $B \times \nabla T$ heat flux dominantly appears in the divertor structure near the separatrix. In the present analysis we also confirmed this characteristic. Near the midplane, T_e is high and the temperature gradient along the magnetic field line is small, therefore the effect $B \cdot \nabla T$ has small contribution and is not apparently observed. The effect is seen in the heat channel width near the divertor.

4. Summary and Discussions

In this paper, we applied the 2-D time-dependent transport code (UEDA code) to study the confinement in SOL plasma of JFT-2M tokamak. The 2-D profiles of density, temperature, surrounding neutrals etc. were caluculated. Using the model transport coefficients, which are anomalous and classical for perpendicular and parallel directions, respectively, we studied the scaling relations of SOL plasma. The plausibility of adopting the model transport coefficient, $D_\perp$, has been discussed on D-III(Ueda et al., 1988) and on JET(Stangeby et al., 1987; Tagle et al., 1987; Erents et al., 1988).

The scaling study of density and tempearure on particle flux and on heat flux were done both at the plasma boundary and at the divertor plate. Simulation results were compared with 1-D calculation and with the theoretical estimates. With respect to the edge temperature, we find a fairly good agreement between our direct simulation and the theoretical estimate. The difference is seen in the heat channel width, λ_T. The power and density dependences are slightly different(see Eq.(3-3) and Eq.(3-5)), which may be due to 2-D effect. Recently, the relation of edge temperature to edge density has been empirically obtained, i.e., $T_e \propto n_e^{-0.4}$ for various ASDEX discharges (Kaufmann et al., 1989). When the power dependence of λ_T will be found experimentally, the difference due to 2-D effect will further be studied.

Using the obtained scaling relations, Eqs.(3-1) and (3-6), we consider the divertor performance and the core confinement. The cold divertor condition in a stationary phase is derived from

Eq.(3-8). Neglecting a radiative cooling term, we have the relation as $\bar{T}_d = P_{out}/\gamma G\Gamma_{out}$. The value of Γ_{out} from the plasma is simply evaluated by the particle confinement time of the core, τ_p, as $\Gamma_{out} \equiv \langle n\rangle V_p/\tau_p$, where V_p is the plasma volume and $\langle n\rangle$ is the averaged density. This leads to $\bar{T}_d = P_{out}\tau_p/\gamma G n V_p$. If we use an empirical law, $\tau_p \simeq 0.05 P_{MW}^{-1/2} n_{e20}^{-1} I_p^0$(P in MW, $\langle n\rangle$ in $10^{20}m^{-3}$), which is obtained in particle control experiment in JT-60 of diverted configuration (Tsuji et al., 1987; Nakamura et al., 1988), we obtain $\bar{T}_d \propto P^{1/2}/\langle n\rangle^2$. This naturally leads to the fact that the high density opeartion is essential in high power regime in order to guarantee the divertor performance.

We do not take into account all the neoclassical effect on the transport coefficients, which may modify the structures of the SOL plasma. In particular, the width of the heat channel is surely modified by the $\nabla T_e B$ heat flux. The inclusion of complete neoclassical effect is left for our future work. We have not yet examined the other transport coefficients than Bohm-like model, the comparison study is necessary to improve model transport coefficients.

When the inclination of the magnetic field to the divertor plate is arbitrary angle, the effect of the secondary emission changes in a complicated manner (Chodura 1984). We discuss the sensitivities of n_d and T_d to the change of the inclination of the magnetic field line and to the neglection of the secondary electron emission. We have examined a special case in the text where the inclination is vary small. In this case, T_d will decrease at most 25%, while n_d may increase by factor of 3 for 5°

$<\phi<10^{\circ}$, if the coefficient of the secondary emission is taken to be 0.8. On the other hand, in the case where the field line is close to perpendicular to the plate ($\phi \sim 90^{\circ}$), the secondary emission dominantly affects the value of transmission coefficient. The normalized velocity of electrons remains almost unchanged. Therefore the neglection of the secondary emission causes the over-estimate of T_d and the under-estimate of n_d. The value of 0.5 (or 0.8) for the secondary emission coefficient causes the over-estimate of T_d by 20% or($\sim$factor 3) and the under-estimate of n_d by 30% (or $\sim$foctor 2). In the intermediate angle, the estimation becomes complicated but the relative deviations are intermediate values between those of two extreme cases ($\phi \simeq 0^{\circ}$ and $\phi \simeq 80^{\circ} \sim 85^{\circ}$). We have not examined the other cases in the simulation. Improvement of the boundary condition is left for future. In addition, further comparison study of the choice of the boundary condition (2-2) with experimental data is surely necessary. With respect to the neglection of the ion conduction part, we have not analysed the other conditions. This model check is important but is left for the future.

In reactor concept, the ash exhaust and impurity problems are other important issues to be persued (Braams, 1987; Brooks, 1987; Itoh, et al., 1988), the analysis on which is beyond the scope of this paper.

Acknowledgements

The authors wish to acknowledge Drs. A. Ehrhardt and D.E. Post for kind permission to use DEGAS code. They also thank Drs.

A. Fukuyama, T. Takizuka for fruitful discussions and comments, Mr. M. Tanaka of Century Research Center for his enthusiastic aid in computation, Drs. N. Asami and M. Nishikawa for their support and Prof. A. Iiyoshi for encouragements. The authors wish to express a special thank to the referee of the journal who kindly helped us to improve this paper. Computations are made on CRAY-1 computer. This work is partly supported by Grant-in-Aid for Fusion Research and Gran-in-Aid for Scientific Research of MoE Japan. A part of work has also been done through the collaboration between universities-JAERI (Japan Atomoc Energy Research Institute) on fusion research.

References

B.J. Braams, in Proceedings of 11th European Conference on Controlled Fusion and Plasma Physics (Aachen, 1983), Part II7D, p 431.

B.J.Braams, M.F.A. Harrison, E.S. Hoston and J.G. Morgan, in Plasma Physics and Controlled Nuclear Fusion Research (London, Sept. 1984) vol.2, IAEA, Vienna, (1985) 125.

B.J. Braams, "A Multi-fluid code for simulation of the edge plasma in tokamaks" NET Report EUR-FU/XII-80/87/68 (1987).

S.I. Braginskii, in Review of Plasma Physics (ed. M.A. Leontovich, New York, Consultant Bureau, 1965) vol.1, p 217.

J.N. Brooks J.Nucl.Mater. 145-157 (1987) 837.

R. Chodura, Phys. Fluids 25 (1982) 1628.

R. Chodura, in Physics of the Plasma Wall Interactions in Controlled Fusion (ed. D.E. Post and H. Behrisch, NATO ASI Series B131, Plenum Press, 1984) p.99.

H.F. Dylla, Internal report of Princeton Plasma Physics Lab. (Princeton Univ.) PPPL-2057 (1982).

S.K.Erents, J.A.Tangle, G.M.Mcracken, P.C.Stangeby, L.C.J. M. De Kock , Nucl. Fusion 28 (1988) 1209.

P.J.Harbour and J.G.Morgan, in Proceedings of 11th European Conference on Controlled Fusion and Plasma Physics (Aachen, 1983), Part II 7D, p 427.

F.H. Harlow and J.E. Welch, Phys. Fluids 8 (1965) 2181.

D.B. Heifets, J. Computational Physics 46 (1982) 309.

F.L. Hinton, Nucl. Fusion 25 (1985) 1457.

F.L. Hinton, in Plasma Physics and Controlled Nuclear Fusion Research (IAEA, Nice, Oct. 1988) D-IV-15.

Yu.I. Igitkhanov, A.S.Kukushikin, A.Yu. Pigarov, V.I. Pistunovich and V.A. Pozharov, in Plasma Physics and Controlled Nuclear Fusion Research (London, Sept. 1984) vol.2, IAEA, Vienna, (1985) 113.

ITER Team, ITER Concept Definition vol.2, IAEA, Vienna, (1989) (ITER Documentation Series, No.3).

K. Itoh, N. Ueda, S.-I. Itoh, et al., Jpn. J. Appl. Phys. 27 (1988) L1750.

S.-I. Itoh, A. Fukuyama, T. Takizuka and K. Itoh, Fusion Tech. 16 (1989) 346.

JT-60 Team, "Review of Preliminary Additional Heating Experiments in JT-60 (Aug.- Nov. 1986)", Res. Rep. Japan Atomic Energy Research Institute, JAERI-M 87-009.

M.Kaufmann, W. Sandmann, M. Bessenrodt-Weberplas et al., in Proceedings of 16th European Conference on Controlled Fusion and Plasma Physics (Venice, 1989), Part 13B, p 47.

K. McCormick, Z.A. Pietrzyk, H. Murmann et al., in Proceedings of 16th European Conference on Controlled Fusion and Plasma Physics (Venice, 1989), Part 13B, p 895.

H. Nakamura, et al., Nucl. Fusion 28 (1988) 43.

J. Neuhauser, W. Schneider, R. Wunderlich, K. Lackner and R. Behringer, J.Nucl. Mater. 121 (1984) 194.

J. Neuhauser, M. Bessenrodt-Weberpals et al., Plasma Physics and Controlled Fusion,(1989) " Tokamak edge modelling and comparison with experiments in ASDEX ", to be published.

M. Petravic, D. Post, D. Heifetz, J. Schmidt, Phys.Rev.Lett. 48 (1982) 326.

M. Petravic, D. Heifetz, S. Heifetz and D. Post, J. Nucl. Mater. 128 (1984) 91.(a)

M. Petravic, D. Heifetz, G.Kuo-Petravic and D. Post, J. Nucl. Mater. 128 (1984) 111.(b)

M. Petravic, D. Heifetz and D. Post, in Plasma Physics and Controlled Nuclear Fusion Research (London, Sept. 1984) vol.2, IAEA, Vienna, (1985) 103.

Physics of the Plasma Wall Interactions in Controlled Fusion (ed. D.E. Post and H. Behrisch, NATO ASI Series B131, Plenum Press, 1984) and papers quoted there in.

S. Saito, T. Kobayashi, M. Suguhara, T. Hirayama and N. Fujisawa, Nucl. Fusion 25 (1985) 828.

P.C. Stangeby, J.A. Tangle, S.K. Erents, C.Lowry in Proceedings of 14th European Conference on Controlled Fusion and Plasma Physics (Madrid, 1987), Part 2, p 670.

P. Stott, et al., in Plasma Physics and Controlled Nuclear Fusion Research (IAEA, Nice, Oct. 1988) A-VII-12.

J.A. Tagle, S.K. Erents, G.M. McCracken, R.A. Pitts, P.C. Stangeby, et al., in Proceedings of 14th European Conference on Controlled Fusion and Plasma Physics (Madrid, 1987),

Part 2, p 662.

T. Takizuka, private communication, 1989; (the relation of the total pressures, p_b and p_d, is found by Takizuka).

S. Tsuji and JT-60 Team, in Proceedings of 14th European Conference on Controlled Fusion and Plasma Physics (Madrid, 1987) Part 1, 57.

N. Ueda, M. Kasai, M. Tanaka, S. Sengoku and M. Sugihara, Nucl. Fusion 28 (1988) 1183.

N. Ueda, K. Itoh and S.-I. Itoh, Nucl. Fusion 29 (1989a) 173.

N. Ueda, K. Itoh, S.-I. Itoh, M. Tanaka, M. Hasegawa, T. Shoji and M. Sugihara, J. Nucl. Mater. 162-164 (1989 b) 607.

N. Ueda and M. Tanaka, "Computer Modelling of Boundary Plasmas in Tokamaks", submitted to J. Nucl. Sci. Technol. (1989 c).

K. Uehara, et al., Phys. Fluids 21 (1979) 89.

F. Wagner, et al., Phys. Rev. Lett. 49 (1982) 1408.

F. Wagner and K. Lackner, in Physics of the Plasma Wall Interactions in Controlled Fusion (ed. D.E. Post and H.

Behrisch, NATO ASI Series B131, Plenum Press, 1984) 931.

F. Wagner and ASDEX Team, Nucl. Fusion 25 (1985) 1490 .

S. Yoshikawa, et al., Phys. Fluids 5 (1963) 1506,

Figure Captions

Fig. 1

Geometry of the analysis. The mesh j correponds to the magnetic surface and i stands for the poloidal angle. j=12 indicates the flux tube touching the separatrix magnetic surface. The hached region indicates the divertor plate, and the length ℓ is mesured along this arc from the bottom to the top. The pitch parameter B_p/B_t is shown as a function of i for various values of j (j = 12 for solid line, j = 11 for dotted-dashed line and j = 10 for dashed line).

Fig. 2

Scaling study on particle flux, Γ_{out}, and heat flux, P_{out}, of the edge density, n_b, and the electron temperature, $T_{b,e}$, (measured at the mid-plane) and those at the divertor plate, n_d and $T_{d,e}$. The locations of measured points are shown in 2(a). The range of Γ_{out} is from 2×10^{21}/sec to 9×10^{22}/sec and that of P_{out} is from 0.2 MW to 0.9 MW as is shown in 2(b). The results on n_b, $T_{b,e}$, n_d and $T_{d,e}$ are shown in 2(c), 2(d), 2(e) and 2(f), respectively.

Fig. 3

The 2-D profiles of electron temperature and ion density in SOL are shown in 3(a) and 3(b) for the case of $\Gamma_{out} = 5\times10^{21}$/sec and $P_{out} = 0.8$ MW. The maximum values of T_e and n_i are 70eV and $5\times10^{18}/m^3$ near the mid-plane and decreases to the directions to the wall and the divertor. The intervals of each contour are 5

eV and $10^{18}/m^3$ respectively. The flow pattern is shown in 3(c) the length of the arrow shows the absolute value of the speed. Its scale is also shown. The neutral density profile is shown in 3(d). Two peaks of the density profile are found along the plate. The peak on the outer-side of the torus is higher. The maximum value of the contour is $8\times10^{11}/cm^3$ and is found on the divertor plate. The interval of the contour is $5\times10^{10}/cm^3$. Neutral density decreases towards the core plasma and some are impinging into the core near the separatrix. The calculated D_α emissivity from n_e, T_e and n_0 is also shown in 3(e)[arb. unit]. The 2-D profile is similar to that of n_0.

Fig. 1

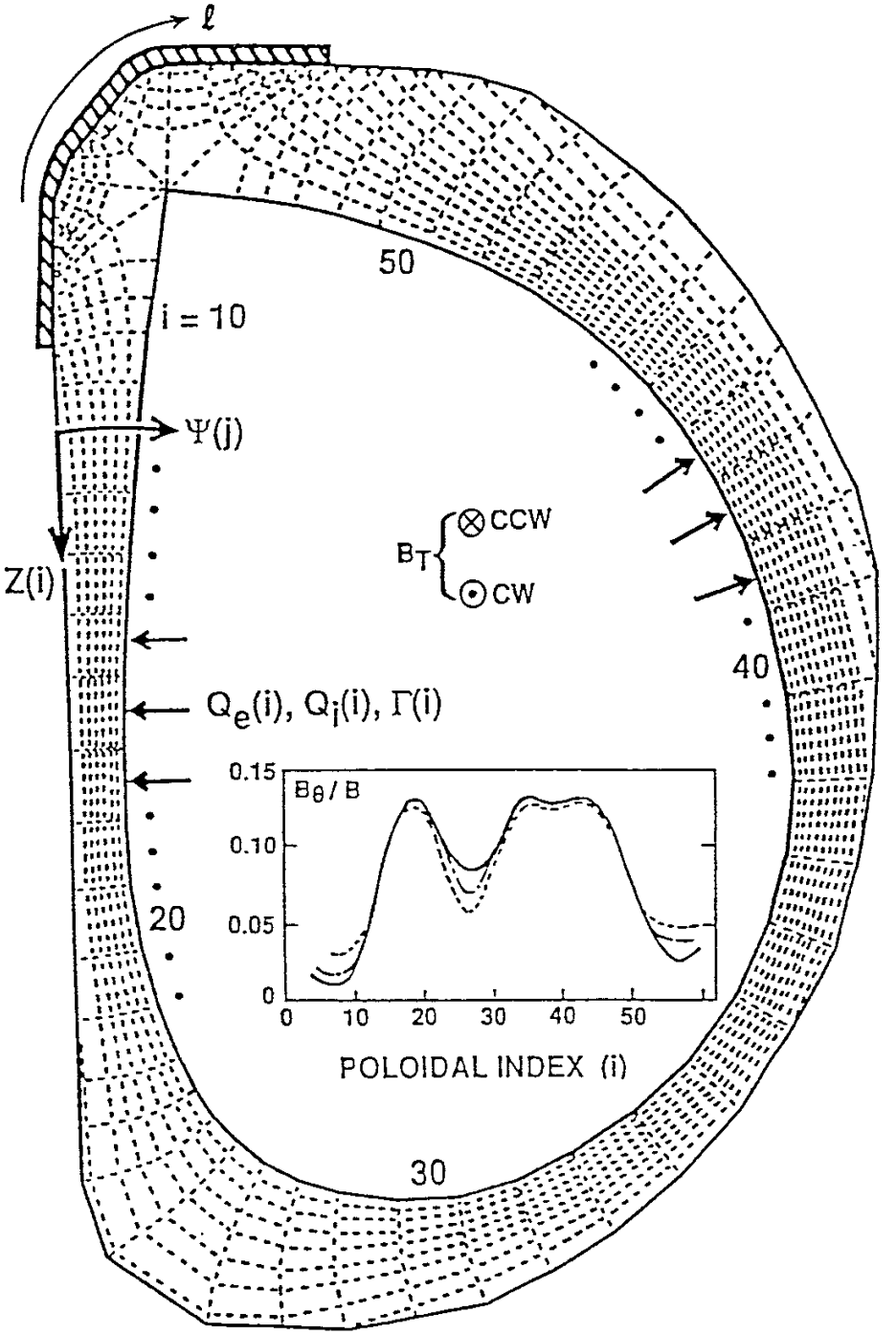
ℓ
50
i = 10
Ψ(j)
Z(i)
B_T ⊗CCW
⊙CW
40
$Q_e(i), Q_i(i), \Gamma(i)$
20
30
B_θ / B
0.15
0.10
0.05
0
0 10 20 30 40 50
POLOIDAL INDEX (i)

Fig. 2

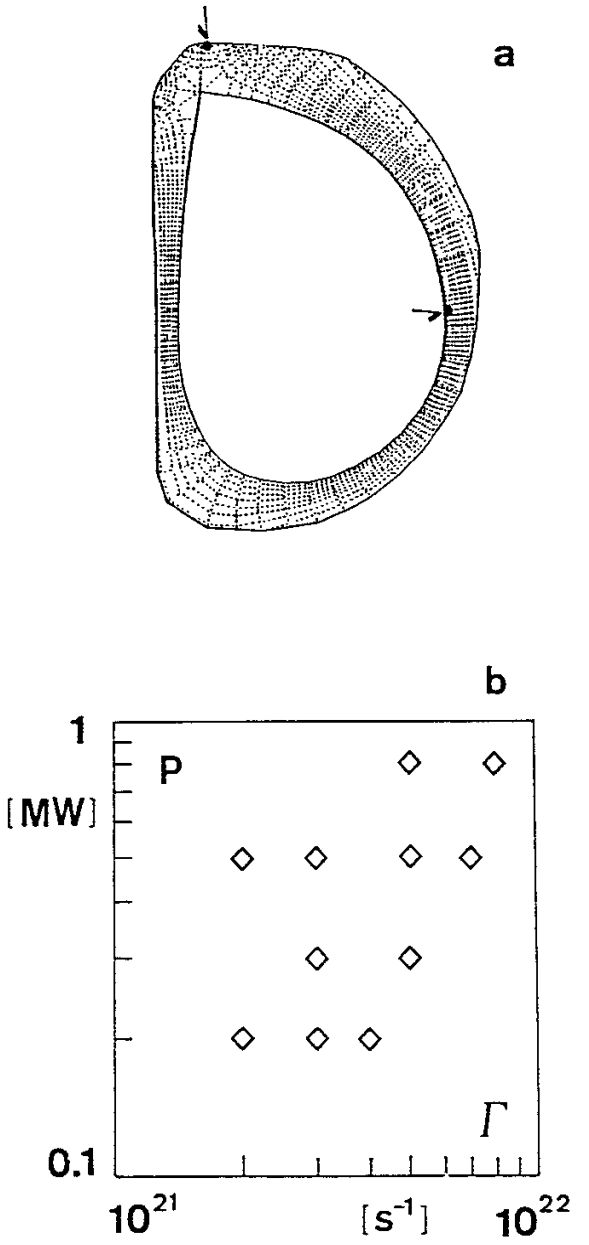

Fig. 2

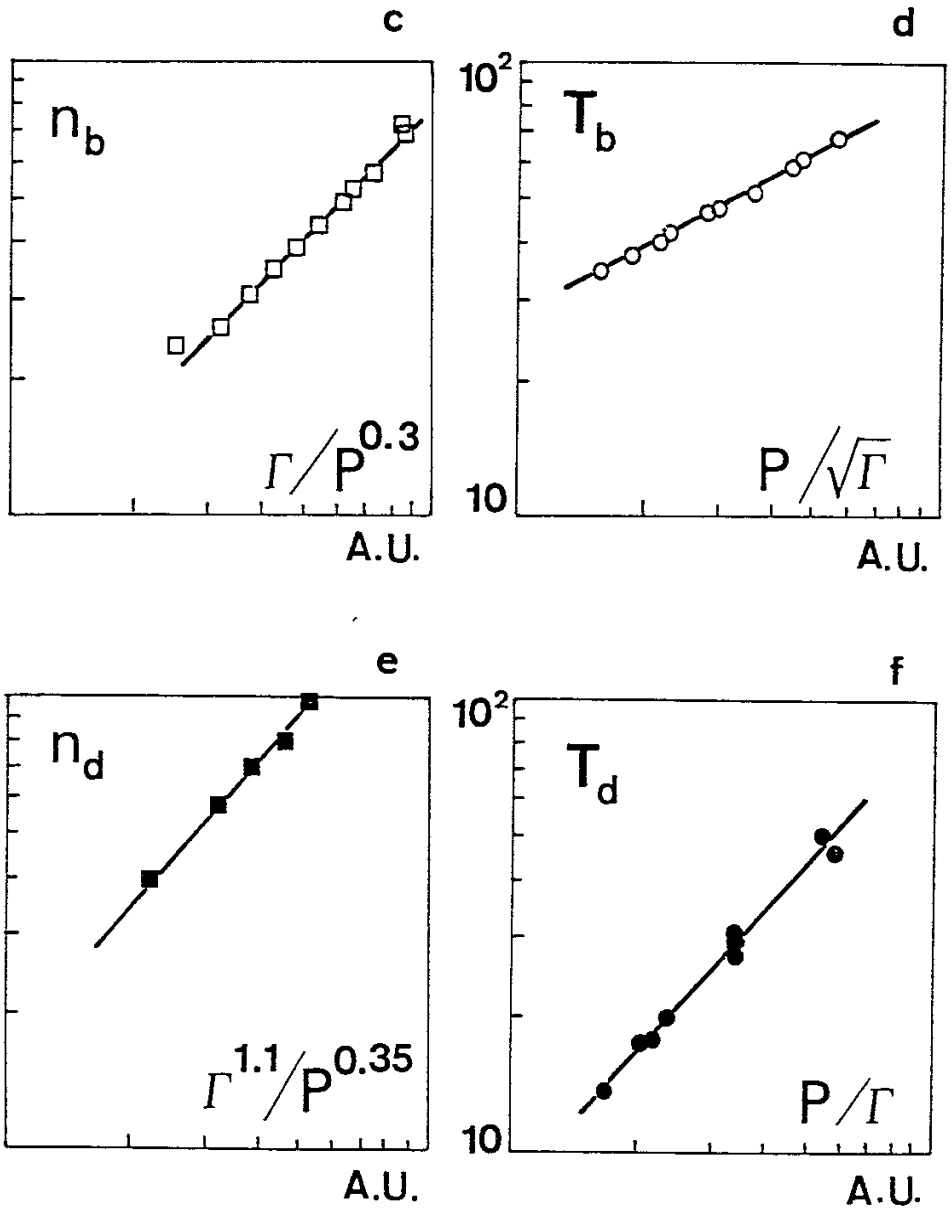
c
d
n_b
10^2
T_b
$\Gamma/P^{0.3}$
$P/\sqrt{\Gamma}$
10
A.U.
A.U.
e
f
n_d
10^2
T_d
$\Gamma^{1.1}/P^{0.35}$
P/Γ
10
A.U.
A.U.

Fig. 3

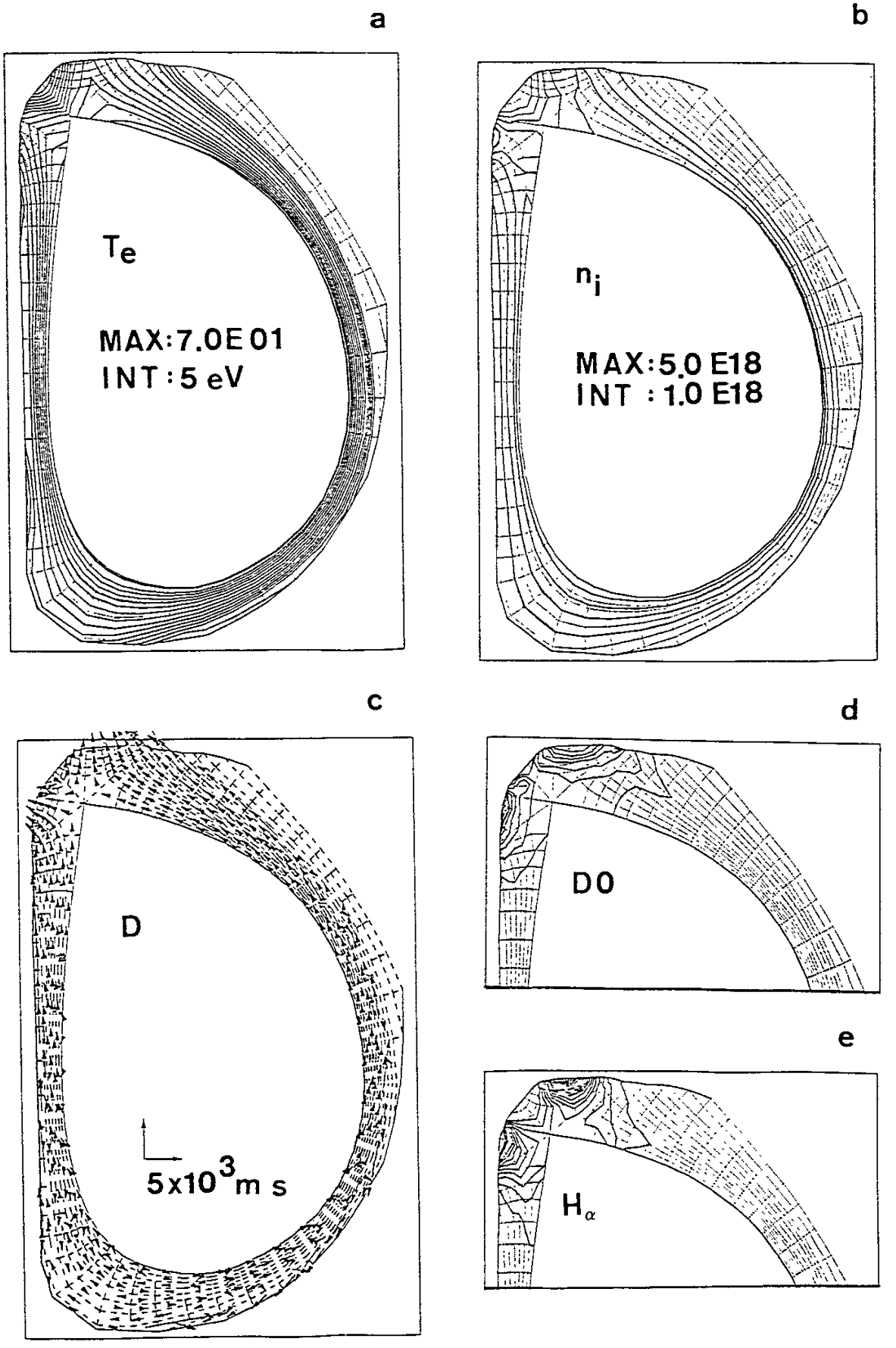
a
b
Te
MAX:7.0E01
INT:5 eV
ni
MAX:5.0 E18
INT : 1.0 E18
c
d
D
D0
5x10^3 m s
e
Hα